

# A mesoscopic device for a realization of the Topological Kondo effect

Saheli Sarkar<sup>1</sup> and Alexei M. Tsvelik<sup>1</sup>

<sup>1</sup>*Division of Condensed Matter Physics and Materials Science,  
Brookhaven National Laboratory, Upton, NY 11973-5000, USA*

The search of anyons is a field of immense interest owing to its potential application in the field of quantum information. Quantum critical Kondo impurities present one possible platform for realization of anyons. In this paper we discuss practical steps for realization of Topological Kondo effect which, in contrast to the well known multichannel Kondo one, remains critical even in the presence of perturbations.

## I. INTRODUCTION

Anyons - fractionalized particles with exotic statistics, are considered an essential part of quantum information systems.<sup>1</sup> There are different suggestions of their realization, one of them being the Kondo effect. Existence of quantum critical Kondo (QCK) effect with a non-Fermi liquid (NFL) behavior, first described and studied theoretically<sup>2-4</sup> has been well established experimentally.<sup>5-9</sup> It is well understood that the corresponding critical ground state contains non-Abelian anyons.<sup>10-12</sup> However, the experiments implement the so-called multichannel Kondo effect where the criticality is sensitive to asymmetry between the scattering channels. Hence a realization of the quantum critical point (QCP) requires a fine tuning of the coupling parameters which limits its potential applications.

Béri and Cooper *et.al.*<sup>13</sup> proposed a new type of non-Fermi liquid Kondo effect where the criticality is stable against most common perturbations. The Topological Kondo effect (TKE) is predicted to arise as a result of coupling between bulk conduction electrons and Majorana Zero modes [MZM, also called Majorana Bound States (MBSs)] located inside of the so-called Majorana-Cooper box (MCB). They also provided a sketch of the MCB setup for TKE<sup>13</sup> in the form of a device consisting of a mesoscopic superconducting island with proximitized to it semiconductor nanowires containing the MBSs. The Coulomb blockade in the island transforms entangled MBSs into an effective quantum spin, which interacts with the conduction electrons of the leads via superexchange interaction facilitating the TKE. In contrast to the conventional QCK effect, the TKE is robust against various perturbations.<sup>14,15</sup>

Apart from being an anyon platform, the TKE with its characteristic features may resolve persistent controversies about the existence of MBS. The theory<sup>13,14</sup> suggests that in the device with  $M$  leads, the linear conductance ( $\sigma_{ij}$ ) between different leads  $i$  and  $j$  saturates at small temperatures at the universal value  $\frac{2e^2}{Mh}$ , following a nontrivial power law temperature dependence, different from the  $T^2$  Fermi liquid one. This universal behavior of the conductance constitutes a manifestation of the anyonic character of the TKE ground state, which therefore can serve as a smoking gun for the presence of MBS.

As we have mentioned above, the suggestions of realization of TKE contained in earlier theoretical studies described heterostructure devices containing nanowires with strong spin-orbit interaction in the presence of magnetic field proximitized to a mesoscopic size superconducting island.<sup>13,15-17</sup> We suggest another route to TKE: to use intrinsic topological

superconductor (TSC)<sup>18-20</sup> based devices, which may naturally host Majorana fermions. This may drastically simplify the fabrication process providing a material realization for the TKE. Promising candidates include iron-based superconductors (FeSC) Fe(Te<sub>x</sub>,Se<sub>1-x</sub>) ( $T_c = 14.5$  K),<sup>21-23</sup> (Li<sub>0.84</sub>Fe<sub>0.16</sub>)OHFeSe ( $T_c = 42$  K)<sup>24</sup> and CaKFe<sub>2</sub>As<sub>4</sub> ( $T_c = 35$  K).<sup>25</sup> All of them exhibit signatures of intrinsic topological superconductivity and have relatively high superconducting critical temperatures  $T_c$ . Thus, it is conceivable that MCB based on such materials can provide a viable path towards observing the TKE. Observation of TKE in turn can serve as a smoking gun signature of MBS, whose detection in various systems has been so far largely focused on observing a zero-bias conductance peak (ZBCP)<sup>26,27</sup> in local probe techniques. Additionally, finding signatures of non-local character<sup>28</sup> of MBS through TKE will be important for quantum computation applications.

The aim of this paper is to provide detailed suggestions for realization of MCBs for TKE focusing on FeSC based systems, with a final goal to use it for quantum information applications. The rest of the paper is organized as follows. In section II, we provide different scenarios for realizing MCBs using FeSC. In section III, we present a FeSC based mesoscopic device and the corresponding parameters characterizing the device for realizing TKE in more realistic experimental situations. In section IV, we depict an arrangement for a TKE-based chiral Kondo lattice which contains multiple non-Abelian anyons. Section V contains a summary.

## II. DIFFERENT SCENARIO FOR REALIZATION OF MAJORANA-COOPER BOXES

There are multiple experiments indicating a possible existence of MBSs in various iron-based superconductors. Non of them are decisive, but as we suggest, in the context of TKE the corresponding systems may provide smoking gun evidence for MBS. Below we consider different arrangements weighting their merits as possible candidates for realization of TKE. In all cases the corresponding MCBs are conceived as mesoscopic devices consisting of superconductor with charging energy  $E_C$  containing MBSs.

### A. Vortices

One way of coexistence of MBSs and superconductivity is through vortices. There are multiple observations of ZBCP trapped in vortex cores of superconductors  $\text{Fe}(\text{Te}_x, \text{Se}_{1-x})$ ,<sup>21–23</sup>  $(\text{Li}_{0.84}\text{Fe}_{0.16})\text{OHFeSe}$ <sup>24</sup> and  $\text{CaKFe}_2\text{As}_4$ .<sup>25</sup> These experiments are interpreted as evidence for MBS. However, there are several difficulties in clearly distinguishing the MBSs, for e.g. due to the presence of topologically trivial Caroli-de Gennes- Matricon (CdGM)<sup>29</sup> states at the vortex cores. The CdGM states are observed to produce a broad peak centering at the zero energy, as the energy separation between the states is of the order of  $\Delta^2/E_F$ , where  $E_F$  is the Fermi energy. Thus as the energy separation can be significantly smaller than the instrumental energy resolution, they appear as a broad peak at the zero energy, being different in origin from that of the MBS. Moreover, scanning-tunneling microscopy (STM) experiments<sup>23,30</sup> in  $\text{FeSe}_{0.45}\text{Te}_{0.55}$  have reported the presence of the ZBCP only in a fraction of the vortex cores present in the system, depending on the magnetic field, rendering the MBSs questionable.

### B. Magnetic point defects

Quantum anomalous vortices<sup>31</sup> may nucleate at magnetic impurities at zero magnetic field. In the presence of a surface topological superconductivity they can support MBSs at the vortex centers, manifesting themselves as ZBCP in tunneling experiments. These types of sharp zero energy peaks located at interstitial iron impurities (IFI) have been observed by (STM) in the superconducting state of  $\text{Fe}_{1+x}(\text{Te}, \text{Se})$ <sup>26</sup> with superconducting gap of about 2 meV, below superconducting temperature  $T_c = 14.5$  K. The zero bias peak intensity decays exponentially from the center of the peak with correlation length  $\xi \approx 3.5$  Å, which is much smaller than the superconducting correlation length  $\sim 25$  Å. The STM have found IFIs on the exposed (*Te*, *Se*) surface located right at the mid position between four neighboring (Te,Se) atoms. They manifest themselves as sharp peaks at zero bias; the peaks remain robust in applied magnetic field up to 8 T. Similar ZBCP have also been found later in  $\text{LiFeAs}$ <sup>32</sup> and in IFI on monolayers of FeSe and  $\text{FeSe}_{0.5}\text{Te}_{0.5}$  on  $\text{SrTiO}_3(\text{STO})$ .<sup>33</sup> One potential problem is that the peak has an intrinsic width in all of the systems [for e.g., in  $\text{Fe}_{1+x}(\text{Te}, \text{Se})$ <sup>26</sup> the width  $\sim 0.6$  meV at  $T = 1.5$  K] whose origin is unclear. Perhaps, this widening can be taken into account phenomenologically as a result of a coupling of the MBS to the bath. In any case, it will likely to have a damaging effect on TKE. Additionally, in a STM experiment<sup>34</sup> in  $\text{FeSe}_{0.45}\text{Te}_{0.55}$  with IFI, the ZBCP was found only near some iron adatoms, the rest of them having Yu-Shiva- Rusinov (YSR) bound states at finite energies.

### C. Line defects

The STM study<sup>35</sup> reports a discovery of zero-energy bound states simultaneously appearing at both ends of a

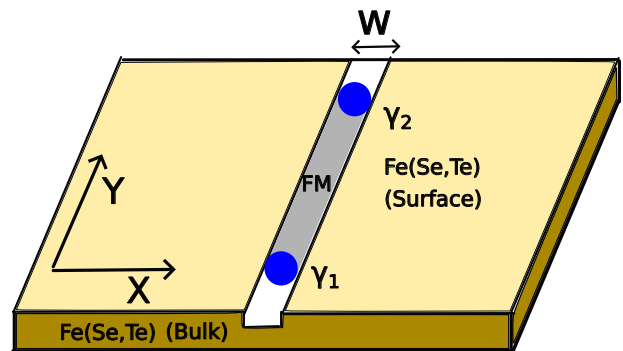


FIG. 1: A schematic representation of a mesoscopic setup for the formation of a paired Majorana bound states: The device contains a slab of  $\text{Fe}(\text{Se}, \text{Te})$  superconductor and a ferromagnetic film (FM) of width  $W$  deposited on the surface of the superconductor, with  $W$  being much smaller than the size of the superconductor. This effectively gives rise to a superconductor-ferromagnet-superconductor (S-F-S) junction.

one-dimensional atomic line defect in monolayer iron-based high-temperature superconductor  $\text{FeTe}_{0.5}\text{Se}_{0.5}$  films grown on  $\text{SrTiO}_3(001)$  substrates, which has  $T_c \approx 62$  K. These line defects naturally emerge during the growth process and correspond to lines of missing Te/Se atoms.

Another recent STM<sup>36</sup> study has found evidence of Majorana fermions in a certain type of crystalline domain walls associated to the half-unit cell shift of the Se atom in superconducting  $\text{FeSe}_{0.45}\text{Te}_{0.55}$  [ $\text{Fe}(\text{Se}, \text{Te})$ ]. It was established in,<sup>37</sup> this material also develops surface ferromagnetism. The first principle calculations<sup>38</sup> have suggested that these types of crystalline domain walls can develop an in-plane ferromagnetism along the domain wall orientation and may support Majorana modes. Moreover, it has been also suggested, that if the magnetization can be tuned, MBS can be trapped by defects such as ferromagnetic domain wall.<sup>38</sup>

Motivated by these, we consider a model device consisting of a mesoscopic  $\text{Fe}(\text{Se}, \text{Te})$  and a ferromagnetic film, which can be used to study TKE with a higher Topological Kondo temperature scale, thus providing advantage of previously proposed setup based on complex heterostructures.

Below we describe in detail the setup of a device giving rise to a pair of MBS's. It is composed of a slab of  $\text{Fe}(\text{Se}, \text{Te})$  material and a thin ferromagnetic film (FM) deposited on the surface of the  $\text{Fe}(\text{Se}, \text{Te})$  or any similar material as shown in the Fig.1. Below the  $T_c$ , one part of the device becomes superconducting, in the thin film area, however, the ferromagnetism persists. Hence, the system can be simply modeled as a superconductor-ferromagnet-superconductor (S-F-S) junction [see Fig.1]. In the Fig. 1, the x-axis points to the normal to the junction between the ferromagnet and the superconductor, where as the y-axis points parallel to the orientation of the junction. The semi-infinite superconducting regions occupy intervals  $x < -W/2$  and  $x > W/2$ , while the FM region occupies interval  $-W/2 < x < W/2$ . We consider that the system size along y-direction as infinite, the width  $W$  remains

finite. The Fe(Se,Te) is known to have non-trivial topological spin-helical Dirac surface states<sup>22</sup> as well as the Rashba type spin-orbit coupling.<sup>39,40</sup> The bulk of Fe(Se,Te) possesses a node-less and almost isotropic s-wave type superconducting gap.<sup>41</sup> The FM produces an effective Zeeman field  $h_y$  parallel to the junction.

Consequently, the surface S-F-S junction of width  $W$  is described by the following Dirac-Bogolyubov-de Gennes (BdG) Hamiltonian<sup>38</sup> in the Nambu basis  $\Psi = (\psi_{k,\uparrow}^\dagger, \psi_{k,\downarrow}^\dagger, \psi_{-k,\uparrow}, \psi_{-k,\downarrow})$ :

$$H_{BdG} = \begin{pmatrix} H_0(k) & i\sigma_y \Delta(r) \\ -i\sigma_y \Delta^*(r) & -H_0^*(-k) \end{pmatrix} \quad (1)$$

In Eqn.(1),  $H_0(k)$  is a  $2 \times 2$  matrix,  $H_0(k) = H_{SO} - \mu + H_Z(x)$ . The  $H_0(k)$  contains the Rashba spin-orbit coupling term  $H_{SO} = \alpha(\boldsymbol{\sigma} \times \mathbf{k}) \cdot \hat{z}$ , associated to the Dirac surface states of the Fe(Se,Te), a chemical potential  $\mu$  and a Zeeman energy term due to the FM given by  $H_Z(x) = \sigma_y h_y \Theta[(W/2) - |x|]$ . Here,  $\alpha = v_F \hbar$ , is the coupling strength, and  $v_F$  is the Fermi velocity.  $\sigma$  are the Pauli matrices in the spin- space. With  $\hbar = 1$ , the Rashba term  $H_{SO}$  becomes  $v_F(\sigma_x k_y + i\sigma_y \partial_x)$ , where  $k_y$  is momentum along the  $y$ -direction that is conserved in the system. The spatial variation of the superconducting gap function on the surface satisfies  $\Delta(r) = \Delta_0 e^{i \text{sgn}(x)(\theta/2)} \Theta[|x| - W/2]$ , where  $\theta$  is the phase difference between the left and the right superconducting regime.

It has been shown in,<sup>38</sup> that the S-F-S junction described by the Hamiltonian Eqn.(1) can support one dimensional counter propagating Majorana modes for a constant phase difference ( $\Delta\phi = \pi$ ) between the two superconducting regimes on the left and right arising due to the in-plane magnetic moment in the FM. Moreover, the localized MBSs are formed<sup>42</sup> from the coupling between these dispersive Majorana modes, if the phase difference  $\Delta\phi(y)$  varies continuously along the orientation  $y$  of the junction such that,  $\Delta\phi(y)$  becomes an odd integer multiple of  $\pi$ . This follows from the analysis of the low energy effective Hamiltonian derived from the BdG Hamiltonian Eqn.(1), by projecting it onto the basis of the one-dimensional Majorana modes.<sup>38</sup>

$$H_{eff} = v_m k_y \tau_y - \Delta_0 \cos \left[ \frac{\Delta\phi(y)}{2} \right] \tau_z, \quad (2)$$

where,  $v_m = v_F \left[ \cos k_F W + \frac{\Delta_0}{\mu} \sin k_F W \right] \frac{\Delta_0^2}{(\mu^2 + \Delta_0^2)}$ ,  $\Delta\phi(y) = \frac{2h_y W}{v_F}$  and  $\tau$  are the Pauli matrices in the particle-hole space. Note that the Eqn.(2) has the form of a Su-Schrieffer-Heeger model. It is also well-known from the Jackiw-Rabbi problem, that a zero energy localized MBS forms when the mass term  $\Delta_0 \cos(\frac{\Delta\phi(y)}{2})$  in Eqn.(2) smoothly changes sign or  $\Delta\phi(y)$  becomes an odd integer multiple of  $\pi$ . The Bogoliubov quasiparticle operator associated with this state is a Majorana fermion, which satisfies  $\gamma_0 = \gamma_0^\dagger$ .

Therefore in this setup, to tune the phase difference  $\Delta\phi(y)$  for obtaining a pair of MBSs, either the width  $W$  of the FM

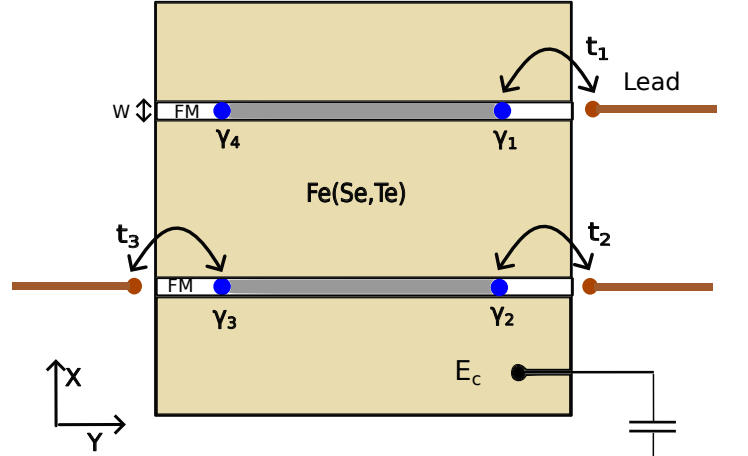


FIG. 2: A schematic representation of a mesoscopic setup for Topological Kondo effect with  $N = 4$  MBSs and  $M = 3$  metallic leads: The device contains a Coulomb blocked superconducting island made of Fe(Se,Te) superconductor and FM. The island is connected to the ground through a capacitor and hence possesses a charging energy  $E_c$ . 3 MBSs are tunnel coupled to the metallic leads with coupling constants  $t_j$ 's ( $j = 1, 2, 3$ ).

can be changed along the  $y$  direction or a soft magnetic material for the FM can be used where one can vary the magnetization strength  $h_y$ .

### III. A $FeSC$ -BASED DEVICE FOR OBSERVATION OF TOPOLOGICAL KONDO EFFECT

The MCB device considered in our work for the realization of the Topological Kondo effect (TKE) comprises of a mesoscopic Fe(Se,Te) (or a similar material) and two ferromagnetic films deposited on it and resulting in a pair of MBS in each of the ferromagnetic films as shown in Fig. 2. Realization of the TKE suggested in the Ref.<sup>13</sup> is based on the MCB which was described, for example, in,<sup>43</sup> containing  $N \geq 4$  MZMs. Following the suggestions, we consider a floating mesoscopic MCB island, grounded through a capacitor. To get the critical ground state, one needs to connect MZMs to just three external metallic leads (this is a minimal number) via tunneling contacts as schematically depicted in Fig. 2. The charging energy  $E_c = \frac{e^2}{2C}$ , with  $C$  being the geometric capacitance of the box, contributes to the Hamiltonian of the MCB island as

$$H_c = E_c(2N_c - Q_0)^2; \quad 2N_c = i\partial/\partial\phi. \quad (3)$$

In Eqn.(3),  $N_c$  is the number of Cooper pairs in the island,  $\phi$  is the phase of the superconducting order parameter, and  $Q_0$  is the background charge determined by the voltage across the capacitor, connected to the MCB.

In general, if there are a total  $N$  number of MBS in the MCB, there will be  $N/2$  number of zero energy fermionic

modes. As the total charge of the island is fixed by a large charging energy  $E_c$ , to even or odd number, thus gives a parity constraint to the MBS operators. This leads to a ground state of the system with  $2^{(N/2)-1}$  fold degeneracy. In this work, we consider the arrangement where MCB island contains four Majorana zero modes  $N = 4$ , hence the ground state is two-fold degenerate. The two degenerate quantum ground states,  $|\downarrow\rangle$  ( $|\uparrow\rangle$ ), have  $N_0$  ( $N_0 - 2$ ) particles in the condensate and empty (filled) pairs of Majorana modes, thus encoding a qubit.<sup>13,44</sup> It is this topological degeneracy which will lead to the effective spin degeneracy for the effective Kondo model. Now, we assume, no overlap between the MBS, hence the degeneracy remains exact, otherwise a ‘‘Zeeman coupling’’<sup>15</sup> term can arise.

The TKE occurs when the MCB is coupled to conduction electrons through external metallic leads as shown in Fig. 2. We work at the energy scales much smaller than the superconducting gap, as well as below the energies of any other subgap excitations of non-Majorana character. In this case the Hamiltonian of the system is given by  $H_{TK} = H_{cond} + H_c + H_{tun}$ , where  $H_{cond}$  is the Hamiltonian of the conduction electrons of the leads. The tunneling Hamiltonian  $H_{tun}$  describes the low-energy coupling between the leads and the MCB island.  $H_{tun}$  is given by

$$H_{tun} = \exp(i\phi/2) \sum_{j=1}^3 t_{jj} \gamma_j \psi_j + \text{H.c.}, \quad (4)$$

where  $\phi$  is the phase of the superconducting order parameter,  $t_{jj}$  is the tunneling amplitude,  $\psi_j$  is the electron annihilation operator and  $\gamma_j$  is the Majorana operator at lead  $j$ . Such tunneling process explicitly excludes the possibility of exciting quasiparticles.<sup>45</sup> As was demonstrated in,<sup>13,46</sup> if the charging energy of the box is much greater than the characteristic value of the tunneling matrix elements, i.e. if  $E_C \gg t_j$ , one can integrate out the phase fluctuations of the condensate which results in the exchange interaction between such MCB and the electrons of the leads (it is supposed that they are spin polarized):

$$H_{ex} = J_K^{ij} (\psi_i^+ \psi_j - \psi_j^+ \psi_i) \gamma_i \gamma_j, \quad J_K^{ij} \sim t_i t_j / E_C, \quad (5)$$

where indices  $i, j$  correspond to the leads. For a single MCB this interaction gives rise to the TKE, where the leads serve as the bulk. The spin operator  $S^i$  realized by the Majorana operators is

$$S^i = \frac{i}{2} \epsilon_{ijk} \gamma_j \gamma_k, \quad \{\gamma_k, \gamma_j\} = \delta_{jk}. \quad (6)$$

The model comprised of the lead Hamiltonian and the effective exchange Hamiltonian [Eqn.(5)] defines an antiferromagnetic Kondo problem.

The Topological Kondo temperature  $T_K$  at which the perturbative approach breaks down due to the RG flow towards strong coupling is given by,<sup>13-15</sup>

$$T_K \sim E_c \exp(-1/\rho \bar{J}_K), \quad (7)$$

where  $\rho$  is the density of states of the lead electrons at the Fermi energy and  $\bar{J}_K$  is the average value of the exchange coupling. Consequently,  $T_K$  sets an energy scale between the trivial regime and the Topological Kondo regime, below which a robust non-Fermi liquid (NFL) behavior can be observed.

One problem is that in all cases apart from tunneling into MBS (4) there may be a direct tunneling of bulk electrons into the superconductor. There are, however, reasons why this process is irrelevant. Indeed, the corresponding Hamiltonian is

$$H_{tun,2} = g \left[ A_{lj} \exp(i\phi) \psi_l \psi_j + \text{H.c.} \right], \quad A_{lj} = -A_{jl}. \quad (8)$$

When we integrate over  $\phi$ , however, the result is a local four fermion interaction which is highly irrelevant.

Below we give estimates of the parameters pertinent to the realization of TKE for the device setup depicted in Fig.2.

We start by summarizing the criteria to be satisfied are: (i) four well-localized MBS, (ii) the MBS must be well-separated, such that the hybridization between them is insignificant, (iii) a charging energy  $E_c$  of the order of the superconducting gap  $\Delta$ . We first evaluate the decay length ( $\lambda$ ) of the MBS wave function inside the ferromagnetic film region. The decay length is given by  $\lambda = \frac{v_m}{\Delta_0}$ .<sup>38</sup> For  $\text{FeSe}_{0.45}\text{Te}_{0.55}$ , with typical values of  $v_F \sim 216 \text{ meV \AA}$ ,<sup>21</sup>  $\Delta_0 \sim 1.8 \text{ meV}$ ,  $\mu \sim 5\Delta_0$  ( $\mu \gg \Delta_0$ ), and considering width of the ferromagnetic region  $W \sim 10 \text{ nm}$ , the decay length is found to be  $\lambda \sim 5 \text{ \AA}$ .

With a superconducting island of area  $A \sim 60 \text{ nm} \times 60 \text{ nm}$  and thickness  $d \sim 1 \text{ nm}$ , and assuming permittivity of an insulating material being  $\epsilon \sim 2 \times 55e^2ev^{-1}(\mu m)^{-1}$ , the charging energy  $E_c = \frac{e^2}{2C}$ , with  $C = \frac{\epsilon A}{d}$  will be of the order of  $1.38 \text{ meV} \equiv 16K \sim \Delta_0$ . Therefore, we see that a mesoscopic MCB island with well-separated and localized MBS can be achieved with a large  $T_K$  [Eqn.(7)]. As the  $T_K$  achieved in the  $\text{Fe}(\text{Se},\text{Te})$  based device can be significantly higher than the heterostructures systems based on semiconductor nanowire and conventional superconductors,<sup>13</sup> this device will significantly improve the experimental feasibility of the TKE.

As we have mentioned in the introduction, that one possible way to detect the TKE is to measure the conductance between different leads, as the TKE leads to unusual temperature dependencies for the two-terminal linear conductance  $\sigma_{ij}$  ( $i \neq j$ ).<sup>14,15</sup> In the temperature-regime larger than  $T_K$ , the  $\sigma_{ij}$  grows as  $\frac{1}{\ln^2(T/T_K)}$  with lowering the temperature. For temperature-regime smaller than  $T_K$ ,  $\sigma_{ij}$  approaches the universal value  $\frac{2e^2}{3h}$  with  $(T/T_K)^{2/3}$  temperature dependence. Both the universal value and the temperature dependence of the conductance are unique characteristics of the NFL ground state providing an alternative pathway for detecting the Majorana fermions in the  $\text{Fe}(\text{Se},\text{Te})$  based device.



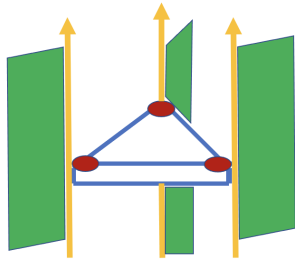


FIG. 3: A schematic depiction of the arrangement for the Chiral Kondo effect. The triangle is the superconducting (Cooper pair) box, the red dots are Majorana zero modes coupled by tunneling to chiral edges of topological insulators.

#### IV. ARRAYS OF TKE

We conclude our paper with a brief description of a device which can incorporate multiple anyons. This is chiral Kondo lattice first described in.<sup>10,47,48</sup> Here the itinerant electrons are chiral, they move in one direction and hence such lattice does not have Ruderman–Kittel–Kasuya–Yosida (RKKY) interaction. In fact, it is equivalent to the bunch of impurities and as a consequence the ground state remains critical as for the single impurity case.

Chiral Kondo lattice for Topological Kondo effect can serve as a platform for anyon-based quantum computation.<sup>10,47,48</sup>

An elementary block of such Kondo lattice is depicted on Fig.(3). The suitable material for chiral edges containing polarized electrons is  $\text{MnBi}_2\text{Te}_4$ ,<sup>49</sup> which is distinguished by a relatively large bulk gap, allowing one to operate at temperatures of order of several degrees.

#### V. SUMMARY

In this work, we have provided a new potential route to achieve the Topological Kondo effect (TKE) through various iron-based superconductors such as  $\text{FeSe}_{0.45}\text{Te}_{0.55}$  [Fe(Se,Te)] based Majorana-Cooper boxes (MCB). The proposed device set up has two marked differences from the earlier proposals set ups which include heterostructures containing semiconductor nanowires proximitized to conventional superconductors. First, there is a significant enhancement of the Topological Kondo temperature scale and the second, there is a simplification of the device structure.

#### VI. ACKNOWLEDGEMENTS

This work was supported by U.S. Department of Energy (DOE) the Office of Basic Energy Sciences, Materials Sciences and Engineering Division under Contract No. DE-SC0012704.

- <sup>1</sup> C. Nayak, S. H. Simon, A. Stern, M. Freedman, and S. Das Sarma, *Rev. Mod. Phys.* **80**, 1083 (2008).
- <sup>2</sup> P. Nozieres and A. Blandin, *Journal de Physique* **41**, 193 (1980).
- <sup>3</sup> A. Tsvetick and P. Wiegmann, *Zeitschrift für Physik B Condensed Matter* **54**, 201 (1984).
- <sup>4</sup> I. Affleck and A. W. Ludwig, *Nuclear Physics B* **352**, 849 (1991).
- <sup>5</sup> R. Potok, I. Rau, H. Shtrikman, Y. Oreg, and D. Goldhaber-Gordon, *Nature* **446**, 167 (2007).
- <sup>6</sup> A. Keller, L. Peeters, C. Moca, I. Weymann, D. Mahalu, V. Umansky, G. Zaránd, and D. Goldhaber-Gordon, *Nature* **526**, 237 (2015).
- <sup>7</sup> Z. Iftikhar, S. Jezouin, A. Anthore, U. Gennser, F. Parmentier, A. Cavanna, and F. Pierre, *Nature* **526**, 233 (2015).
- <sup>8</sup> Z. Iftikhar, A. Anthore, A. Mitchell, F. Parmentier, U. Gennser, A. Ouerghi, A. Cavanna, C. Mora, P. Simon, and F. Pierre, *Science* **360**, 1315 (2018).
- <sup>9</sup> D. Karki, E. Boulat, W. Pouse, D. Goldhaber-Gordon, A. K. Mitchell, and C. Mora, *Physical Review Letters* **130**, 146201 (2023).
- <sup>10</sup> P. L. S. Lopes, I. Affleck, and E. Sela, *Phys. Rev. B* **101**, 085141 (2020).
- <sup>11</sup> Y. Komijani, *Phys. Rev. B* **101**, 235131 (2020).
- <sup>12</sup> Y. Ge and Y. Komijani, *Phys. Rev. Lett.* **129**, 077202 (2022).
- <sup>13</sup> B. Béri and N. R. Cooper, *Phys. Rev. Lett.* **109**, 156803 (2012).
- <sup>14</sup> A. Altland and R. Egger, *Phys. Rev. Lett.* **110**, 196401 (2013).
- <sup>15</sup> A. Altland, B. Béri, R. Egger, and A. M. Tsvetlik, *Phys. Rev. Lett.* **113**, 076401 (2014).
- <sup>16</sup> J. I. Väyrynen, A. E. Feiguin, and R. M. Lutchyn, *Phys. Rev. Res.* **2**, 043228 (2020).
- <sup>17</sup> D. Liu, Z. Cao, X. Liu, H. Zhang, and D. E. Liu, *Phys. Rev. B* **104**, 205125 (2021).
- <sup>18</sup> C. Beenakker, *Annu. Rev. Condens. Matter Phys.* **4**, 113 (2013).
- <sup>19</sup> M. Sato and Y. Ando, *Reports on Progress in Physics* **80**, 076501 (2017).
- <sup>20</sup> G. Xu, B. Lian, P. Tang, X.-L. Qi, and S.-C. Zhang, *Phys. Rev. Lett.* **117**, 047001 (2016).
- <sup>21</sup> D. Wang, L. Kong, P. Fan, H. Chen, S. Zhu, W. Liu, L. Cao, Y. Sun, S. Du, J. Schneeloch, R. Zhong, G. Gu, L. Fu, H. Ding, and H.-J. Gao, *Science* **362**, 333 (2018).
- <sup>22</sup> P. Zhang, K. Yaji, T. Hashimoto, Y. Ota, T. Kondo, K. Okazaki, Z. Wang, J. Wen, G. Gu, H. Ding, *et al.*, *Science* **360**, 182 (2018).
- <sup>23</sup> T. Machida, Y. Sun, S. Pyon, S. Takeda, Y. Kohsaka, T. Hanaguri, T. Sasagawa, and T. Tamegai, *Nature materials* **18**, 811 (2019).
- <sup>24</sup> Q. Liu, C. Chen, T. Zhang, R. Peng, Y.-J. Yan, C.-H.-P. Wen, X. Lou, Y.-L. Huang, J.-P. Tian, X.-L. Dong, G.-W. Wang, W.-C. Bao, Q.-H. Wang, Z.-P. Yin, Z.-X. Zhao, and D.-L. Feng, *Phys. Rev. X* **8**, 041056 (2018).
- <sup>25</sup> W. Liu, L. Cao, S. Zhu, L. Kong, G. Wang, M. Papaj, P. Zhang, Y.-B. Liu, H. Chen, G. Li, *et al.*, *Nature Communications* **11**, 5688 (2020).
- <sup>26</sup> J.-X. Yin, Z. Wu, J. Wang, Z. Ye, J. Gong, X. Hou, L. Shan, A. Li, X. Liang, X. Wu, *et al.*, *Nature Physics* **11**, 543 (2015).
- <sup>27</sup> S. Zhu, L. Kong, L. Cao, H. Chen, M. Papaj, S. Du, Y. Xing, W. Liu, D. Wang, C. Shen, *et al.*, *Science* **367**, 189 (2020).
- <sup>28</sup> J. Alicea, *Reports on progress in physics* **75**, 076501 (2012).
- <sup>29</sup> C. Caroli, P. De Gennes, and J. Matricon, *Physics Letters* **9**, 307 (1964).
- <sup>30</sup> L. Kong, S. Zhu, M. Papaj, H. Chen, L. Cao, H. Isobe, Y. Xing, W. Liu, D. Wang, P. Fan, *et al.*, *Nature Physics* **15**, 1181 (2019).

- <sup>31</sup> K. Jiang, X. Dai, and Z. Wang, *Phys. Rev. X* **9**, 011033 (2019).
- <sup>32</sup> S. S. Zhang, J.-X. Yin, G. Dai, L. Zhao, T.-R. Chang, N. Shumiya, K. Jiang, H. Zheng, G. Bian, D. Multer, M. Litskevich, G. Chang, I. Belopolski, T. A. Cochran, X. Wu, D. Wu, J. Luo, G. Chen, H. Lin, F.-C. Chou, X. Wang, C. Jin, R. Sankar, Z. Wang, and M. Z. Hasan, *Phys. Rev. B* **101**, 100507 (2020).
- <sup>33</sup> C. Liu, C. Chen, X. Liu, Z. Wang, Y. Liu, S. Ye, Z. Wang, J. Hu, and J. Wang, *Science advances* **6**, eaax7547 (2020).
- <sup>34</sup> P. Fan, F. Yang, G. Qian, H. Chen, Y.-Y. Zhang, G. Li, Z. Huang, Y. Xing, L. Kong, W. Liu, *et al.*, *Nature communications* **12**, 1348 (2021).
- <sup>35</sup> C. Chen, K. Jiang, Y. Zhang, C. Liu, Y. Liu, Z. Wang, and J. Wang, *Nature Physics* **16**, 536 (2020).
- <sup>36</sup> Z. Wang, J. O. Rodriguez, L. Jiao, S. Howard, M. Graham, G. Gu, T. L. Hughes, D. K. Morr, and V. Madhavan, *Science* **367**, 104 (2020).
- <sup>37</sup> N. Zaki, G. Gu, A. Tsvelik, C. Wu, and P. D. Johnson, *Proceedings of the National Academy of Sciences* **118**, e2007241118 (2021).
- <sup>38</sup> R. Song, P. Zhang, and N. Hao, *Phys. Rev. Lett.* **128**, 016402 (2022).
- <sup>39</sup> M. H. Christensen, J. Kang, and R. M. Fernandes, *Phys. Rev. B* **100**, 014512 (2019).
- <sup>40</sup> E. Mascot, S. Cocklin, M. Graham, M. Mashkooi, S. Rachel, and D. K. Morr, *Communications Physics* **5**, 188 (2022).
- <sup>41</sup> S. Sarkar, J. Van Dyke, P. O. Sprau, F. Massee, U. Welp, W.-K. Kwok, J. C. S. Davis, and D. K. Morr, *Phys. Rev. B* **96**, 060504 (2017).
- <sup>42</sup> L. Fu and C. L. Kane, *Phys. Rev. Lett.* **100**, 096407 (2008).
- <sup>43</sup> C.-X. Liu, D. E. Liu, F.-C. Zhang, and C.-K. Chiu, *Phys. Rev. Appl.* **12**, 054035 (2019).
- <sup>44</sup> L. Fu, *Phys. Rev. Lett.* **104**, 056402 (2010).
- <sup>45</sup> S. Plugge, A. Zazunov, E. Eriksson, A. M. Tsvelik, and R. Egger, *Phys. Rev. B* **93**, 104524 (2016).
- <sup>46</sup> M. R. Galpin, A. K. Mitchell, J. Temaismithi, D. E. Logan, B. Béri, and N. R. Cooper, *Phys. Rev. B* **89**, 045143 (2014).
- <sup>47</sup> D. Gabay, C. Han, P. L. S. Lopes, I. Affleck, and E. Sela, *Phys. Rev. B* **105**, 035151 (2022).
- <sup>48</sup> M. Lotem, E. Sela, and M. Goldstein, *Phys. Rev. Lett.* **129**, 227703 (2022).
- <sup>49</sup> Z. Ying, S. Zhang, B. Chen, B. Jia, F. Fei, M. Zhang, H. Zhang, X. Wang, and F. Song, *Phys. Rev. B* **105**, 085412 (2022).